

# Bessel-like optical beams with arbitrary trajectories

Ioannis D. Chremmos,<sup>1,\*</sup> Zhiqiang Chen,<sup>2</sup> Demetrios N. Christodoulides,<sup>3</sup> and Nikolaos K. Efremidis<sup>1</sup>

<sup>1</sup>Department of Applied Mathematics, University of Crete, Heraklion 71409, Greece

<sup>2</sup>Department of Physics and Astronomy, San Francisco State University, San Francisco, California 94132, USA

<sup>3</sup>CREOL/College of Optics, University of Central Florida, Orlando, Florida 32816, USA

\*Corresponding author: jochremm@central.ntua.gr

Received September 27, 2012; accepted October 19, 2012;

posted November 5, 2012 (Doc. ID 177039); published November 30, 2012

A method is proposed for generating Bessel-like optical beams with arbitrary trajectories in free space. The method involves phase-modulating an optical wavefront so that conical bundles of rays are formed whose apexes write a continuous focal curve with pre-specified shape. These ray cones have circular bases on the input plane; thus their interference results in a Bessel-like transverse field profile that propagates along the specified trajectory with a remarkably invariant main lobe. Such beams can be useful as hybrids between non-accelerating and accelerating optical waves that share diffraction-resisting and self-healing properties. © 2012 Optical Society of America

OCIS codes: 050.1940, 260.2030, 350.5500, 070.2580.

Nondiffracting optical beams play an important role in contemporary optics. Two major classes of such beams can be distinguished: nonaccelerating and accelerating. The first class refers to waves whose transverse profile and propagation direction remain invariant. Perhaps the most renowned examples are Bessel beams, which came to light in 1987 [1] and have found numerous applications in micromanipulation, atom and nonlinear optics [2]. Mathieu [3] and parabolic beams [4] are other characteristic counterparts with explicitly known angular spectrums. This class also includes waves that remain invariant in a frame rotating around the propagation axis [5]. The second class is represented by recently discovered nondiffracting beams with the peculiar property to self-accelerate along a parabola. These waves emerged in 2007 with the introduction of Airy beams [6], a concept stimulated by quantum mechanics [7]. Parabolic accelerating beams [8] are another characteristic example. These beams (mostly Airy) have also found several applications for light trajectory control and navigation around objects, micromanipulation, surface plasmon routing, curved plasma filaments and autofocusing (see [9] for a recent review).

Although the two wave families have evolved rather independently, it would be interesting to combine their features toward the design of new wave entities. A possibility would be to design beams with the symmetry and resistance to diffraction of Bessel beams that are also capable of self-acceleration. Moreover, it would be desirable to control the beam trajectory beyond the parabolic law. Although not strictly nondiffracting, such beams could be useful as hybrids between the two classes in applications, such as microfabrication and optical tweezers. Interestingly, few recent works point toward this direction by proposing techniques to create Bessel-like beams with *spiraling* and *snaking* trajectories [10–13].

In this Letter we propose a method for generating Bessel-like beams with arbitrary trajectories. Specifically, we consider the general problem of finding the phase of an input wavefront that directs rays to create an arbitrary focal curve. Any point on this curve is the apex of a conical ray bundle emanating from a circle on the input plane and interfering to create a Bessel-like field pattern that propagates along the specified path.

The beam shows resistance to diffraction keeping its main lobe remarkably invariant.

We consider the paraxial Fresnel integral

$$u(X, Y, Z) = \iint \frac{u(x, y, 0)}{2\pi i Z} e^{i\frac{(X-x)^2 + (Y-y)^2}{2Z}} dx dy, \quad (1)$$

where  $u(x, y, 0) = A(x, y) \exp[iQ(x, y)]$  is the phase-modulated input wavefront with the transverse and longitudinal coordinates being scaled by  $l$  and  $kl^2$ , respectively,  $k$  being the wavenumber, and  $l$  is arbitrary. Our goal is to determine  $Q$  so that a focal curve is created that is parametrically expressed as  $(f(Z), g(Z), Z)$ , where  $f, g$  are given functions. Any point  $F(Z)$  of that curve must be the intersection of a conical ray bundle. Equivalently, from a stationary phase approach to Eq. (1), the first partials of  $Q$  must satisfy  $Q_x = (f - x)/Z$ ,  $Q_y = (g - y)/Z$ , where  $(x, y, 0)$  is the starting point of any ray in that bundle. The continuum of points  $(x, y, 0)$  defines a geometric locus  $C(Z)$  on  $Z = 0$  that can be viewed as the isocurve of a function  $Z(x, y)$ . Now note that, if  $Q$  is to be twice continuously differentiable, its mixed partials should be equal, i.e.,  $Q_{xy} = Q_{yx}$ , yielding  $(x - x_c)Z_y = (y - y_c)Z_x$ , where  $x_c = f - Zf'$ ,  $y_c = g - Zg'$  ( $'$  denotes  $d/dZ$ ). Therefore, along an isocurve,  $\nabla Z$  is collinear to vector  $(x - x_c, y - y_c)$ , which means that  $C(Z)$  is a circle with center  $(x_c, y_c, 0)$  and radius  $R(Z)$  that is arbitrary for the moment. From the expressions of  $x_c, y_c$  it is also obvious that the circle center is the point at which the tangent to the focal curve at  $F(Z)$  intersects the input plane. We are therefore led to a clear physical picture: The continuous focal line is the locus of the apexes of conical ray bundles emitted from expanding and shifting circles on the input plane (Fig. 1).

The circle radius is directly related to the transverse beam profile. To see this, notice that each point  $(x, y, 0)$  of  $C(Z)$  approximately contributes a plane wave to the field around  $F(Z)$ . Neglecting amplitude variations, this contribution can be expressed in the paraxial approximation as  $du = \exp[iP + i(f - x, g - y) \cdot (\delta X, \delta Y)/Z]$ , ( $\cdot$  denotes inner product) where  $(\delta X, \delta Y) = (X - f, Y - g)$  are local focal coordinates and

$$P(Z) = Q(x, y) + [(f - x)^2 + (g - y)^2]/2Z \quad (2)$$

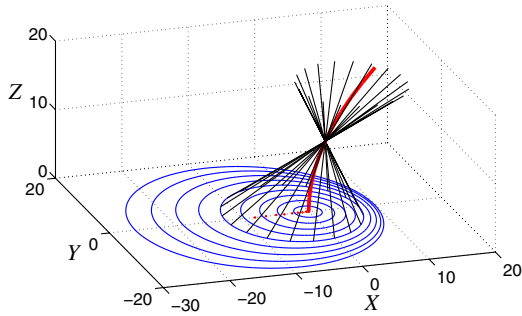


Fig. 1. (Color online) Schematic of the principle: Rays emitted from expanding circles on the input plane intersect on the specified focal curve. The dots are the shifting circle centers.

is constant along  $C(Z)$  due to the phase stationarity imposed on the integrand of Eq. (1). By integrating all  $du$  along  $C(Z)$  and using polar coordinates  $(\delta X, \delta Y) = r(\cos \theta, \sin \theta)$ ,  $(x - x_c, y - y_c) = R(\cos \varphi, \sin \varphi)$ , we end up with  $2\pi K \exp(iP) J_0(Rr/Z)$ , where  $K = \exp[i(f - x_c, g - y_c) \cdot (\delta X, \delta Y)/Z]$  and  $J_0$  is the Bessel function. Therefore, at any  $Z$  plane, the optical field around the focus behaves like a Bessel function modulated by a plane wave. By further choosing  $R(Z) = \gamma Z$ , the Bessel dependence becomes  $J_0(\gamma r)$ , namely independent of  $Z$ , thus imparting to the beam a diffraction-resisting quality. Now, to determine  $P$ , we differentiate Eq. (2) with respect to  $x$  (or  $y$ ) and use the stationarity conditions and the circle equation to obtain

$$P(Z) = \frac{1}{2} \int_0^Z \{ [f'(\zeta)]^2 + [g'(\zeta)]^2 - [R(\zeta)/\zeta]^2 \} d\zeta, \quad (3)$$

where arbitrarily  $P(0) = 0$ . Summarizing, the procedure for computing  $Q$  for given trajectory and radius functions is as follows: For any point  $(x, y, 0)$ , solve the circle equation  $(x - x_c)^2 + (y - y_c)^2 = R^2$  for  $Z$ , and then substitute to Eqs. (3) and Eq. (2) to find  $P$  and  $Q$ , respectively.

The above algorithm is well defined only when the circle equation has a unique solution for  $Z$ , which means that circles  $C(Z)$  corresponding to different  $Z$  must not intersect. This is equivalent to the requirement that  $\nabla Z$  is finite. The gradient can be obtained by differentiating the circle equation and reads  $\nabla Z = (x - x_0, y - y_0)/D$ , where  $D = RR' + (x - x_c)x'_c + (y - y_c)y'_c$ , where  $x'_c = -Zf''$ ,  $y'_c = -Zg''$ . It follows that  $D$  is never zero *if*

$$R'(Z) > Z \sqrt{[f''(Z)]^2 + [g''(Z)]^2}. \quad (4)$$

This condition defines a maximum propagation distance  $Z_m$  at which the focal curve can be created or, equivalently, a maximum circle  $C(Z_m)$  in the exterior of which the above definition of  $Q$  fails. Beyond  $Z_m$ , a different trajectory must be defined. In order that  $Q$  is continuously differentiable on  $C(Z_m)$  and the beam keeps resisting diffraction, we choose to continue the trajectory along its tangent at the ultimate point  $F(Z_m)$  while keeping the same  $R(Z)$ . Then, circles  $C(Z)$  for  $Z > Z_m$  are concentric and centered at  $(x_c(Z_m), y_c(Z_m), 0)$  and the emitted ray cones create a Bessel beam propagating in the direction of vector  $(f'(Z_m), g'(Z_m), 1)$ . The maximum  $Z$  range is determined by the most exterior (largest) cone.

Figure 2 shows an example of a Bessel-like beam with a parabolic trajectory lying on plane  $Y = 0$ . The input condition is the Gaussian  $\exp(-r^2/900)$  modulated by the phase  $Q$  shown in Fig. 2(a). The amplitude evolution on  $Y = 0$  verifies the beam trajectory, which is a parabola up to  $Z_m = 20$  and a straight line thereafter. From the transverse profiles at different distances, the Bessel-like pattern is observed with a remarkably diffraction-resisting main lobe that is an almost perfect fit of  $J_0(r)$  ( $\gamma = 1$ ). Note also how the Bessel rings deform asymmetrically while the beam accelerates. Beyond  $Z_m$ , acceleration stops and the symmetric Bessel profile is restored.

The beam's trajectory can also be defined piecewise. Figures 3(a)–3(c) refer to a beam that initially propagates straight and then is deflected along a half-period cosine to finally return to a straight but parallel to the initial path. The case of a hyperbolic trajectory is shown in Figs. 3(d)–3(f). A hyperbola is asymptotic to a straight line ( $f'' \rightarrow 0$ ); hence its parameters can be chosen so that (4) is satisfied for all  $Z$ . In both cases of Fig. 3 note how accurately the trajectory of the main lobe reproduces the expected analytical curve (dashed line). Also notable is again the resistance of the main lobe to diffraction.

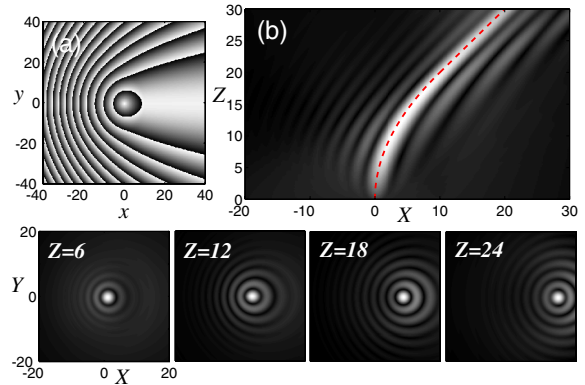


Fig. 2. (Color online) (a) Modulo- $2\pi$  input phase for a Bessel-like beam with trajectory  $f(Z) = Z^2/40$ ,  $g = 0$  and  $R(Z) = Z$ . (b) Evolution of amplitude on plane  $Y = 0$ . Dashed curve is the analytic trajectory. Bottom row: Transverse amplitude profiles at different  $Z$ .

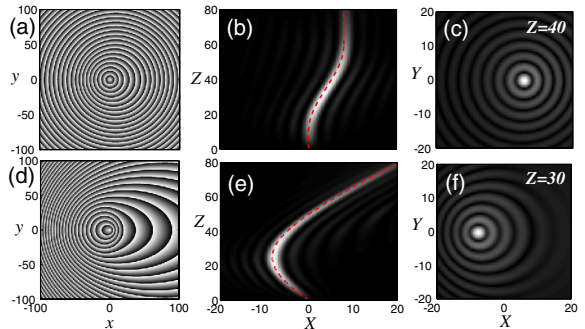


Fig. 3. (Color online) (a) Modulo- $2\pi$  input phase; (b) amplitude evolution on  $Y = 0$ ; and (c) transverse profile at the indicated distance for a Bessel-like beam with a piecewise trajectory. The  $10 < Z < 60$  part of the trajectory is  $f(Z) = 4[1 - \cos(\pi(Z - 10)/50)]$ . (d)–(f) Corresponding results for the hyperbolic trajectory  $f(Z) = (0.64Z^2 - 32Z + 800)^{1/2} - 800^{1/2}$ .  $R(Z) = Z$  for both beams.

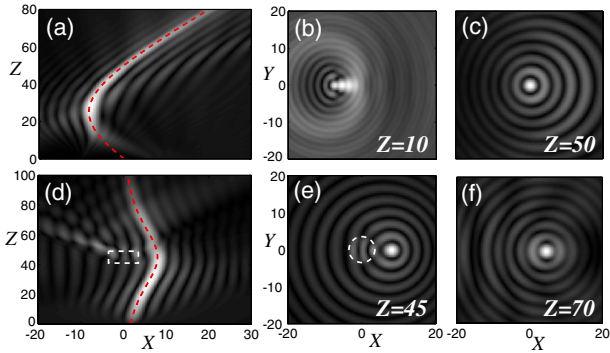


Fig. 4. (Color online) (a)–(c) Self-healing evolution and transverse profiles of the hyperbolic beam of Fig. 3, when a disk with center  $(-10, 0)$  and radius 20 is obstructed on  $Z = 0$ . (d)–(f) A beam with trajectory  $8 \operatorname{sech}[0.05(Z - 45)]$  propagating around a cylindrical potential with strength 0.5 (dashed line).

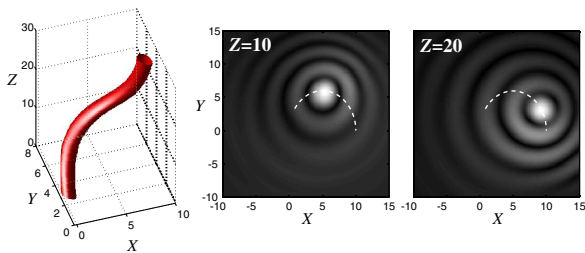


Fig. 5. (Color online) Main lobe track and transverse profiles of a beam with trajectory  $f(Z) = 5 \tanh[0.12(Z - 10)] + 5$ ,  $g(Z) = 6 \operatorname{sech}[0.12(Z - 10)]$ . The dashed curves are the projection of the trajectory on the  $X$ - $Y$  plane.

By virtue of their ray structure, the proposed waves inherit from standard Bessel beams the property to self-reconstruct their profile after being distorted [14]. Figure 4(a) shows the evolution of the beam with hyperbolic trajectory of Fig. 3 after removing a circular disk from its input wavefront. Despite the initial distortion [Fig. 4(b)], the beam profile is fully recovered after some *healing* distance [Fig. 4(c)]. Furthermore, the beams' trajectory can be engineered to guide light around objects. In Fig. 4(d) a beam propagates along a hyperbolic secant path to avoid an on-axis index potential, thus keeping its

main lobe nearly unaffected [Fig. 4(e)]. Finally, the case of a beam with a 3D trajectory is examined in Fig. 5.

In conclusion, we have proposed a method for generating Bessel-like optical beams with arbitrary trajectories. The proposed beams combine the circular profile, resistance to diffraction, and self-reconstructing properties of standard Bessel beams with the ability to accelerate along rather arbitrary paths. Their implementation should be straightforward by phase-modulating a simple optical wavefront via a spatial light modulator and is limited only by the pixelization of the input phase. As hybrids between nonaccelerating and accelerating diffraction-resisting beams, the new waves can find applications in particle manipulation and laser microfabrication.

This work was supported by project ACMAC, FP7-REGPOT-2009-1, and by action "ARISTEIA"—Operational Programme "Education and Lifelong Learning," cofunded by the European Social Fund and National Resources.

## References

1. J. Durnin, *J. Opt. Soc. Am. A* **4**, 651 (1987).
2. D. McGloin and K. Dholakia, *Contemp. Phys.* **46**, 15 (2005).
3. J. C. Gutiérrez-Vega, M. D. Iturbe-Castillo, and S. Chávez-Cerda, *Opt. Lett.* **25**, 1493 (2000).
4. M. A. Bandres, J. C. Gutiérrez-Vega, and S. Chávez-Cerda, *Opt. Lett.* **29**, 44 (2004).
5. R. Piestun and J. Shamir, *J. Opt. Soc. Am. A* **15**, 3039 (1998).
6. G. A. Siviloglou and D. N. Christodoulides, *Opt. Lett.* **32**, 979 (2007).
7. M. Berry and N. Balazs, *Am. J. Phys.* **47**, 264 (1979).
8. M. A. Bandres, *Opt. Lett.* **33**, 1678 (2008).
9. Y. Hu, G. Siviloglou, P. Zhang, N. Efremidis, D. Christodoulides, and Z. Chen, *Self-Accelerating Airy Beams: Generation, Control, and Applications* (Springer, 2012), pp. 1–46.
10. V. Jarutis, A. Matijošius, P. D. Trapani, and A. Piskarskas, *Opt. Lett.* **34**, 2129 (2009).
11. A. Matijošius, V. Jarutis, and A. Piskarskas, *Opt. Express* **18**, 8767 (2010).
12. J. Morris, T. Cizmar, H. Dalgarno, R. Marchington, F. Gunn-Moore, and K. Dholakia, *J. Opt.* **12**, 124002 (2010).
13. S.-H. Lee, Y. Roichman, and D. G. Grier, *Opt. Express* **18**, 6988 (2010).
14. V. Garcés-Chavez, D. McGloin, H. Melville, W. Sibbett, and K. Dholakia, *Nature* **419**, 145 (2002).